compounds and to elucidate the important factors for determining the suitability of a source compound for the formation of desirable thin film materials.

Acknowledgment. We thank Dr. Stephen D. Hersee and Mr. George O. Ramseyer for their technical assistance and valuable discussions during the course of this work. We thank the National Science Foundation (Grant No. MSS-89-09793), International Business Machines, the General Electric Co., and the Wright-Patterson Laboratory (Award No. F33615-90-C-5291) for support of this work.

Registry No. Al, 7429-90-5; AlBn, 37367-77-4; Al_2O_2, 1344-28-1; $Al(BH_4)_3$, 13771-22-7; $AlH_2(BH_4)\cdot N(CH_3)_3$, 92275-85-9.

Chemical Vapor Deposition Precursor Chemistry. 3. Formation and Characterization of Crystalline Nickel Boride Thin Films from the Cluster-Assisted Deposition of Polyhedral Borane Compounds[1]

Shreyas S. Kher and James T. Spencer*

Department of Chemistry and the Center for Molecular Electronics, Center for Science and Technology, Syracuse University, Syracuse, New York 13244-4100

Received July 22, 1991. Revised Manuscript Received February 10, 1992

The deposition of both metal-rich and boron-rich thin-film phases of nickel boride from boron-containing precursor compounds by a cluster deposition process is reported. The thin films were characterized by EDXA, AES, SEM, XRD, FT-IR, TEM, and electron diffraction experiments. The films were shown by AES to be compositionally uniform in the bulk sample. Film thicknesses up to 3 μm were readily prepared by controlling the flow rate of the borane into the cell, the substrate temperature, and the duration of the deposition. The stoichiometric composition of the films was controlled by regulating the deposition temperature, the borane flow rate into the reactor, and the base vacuum conditions during the film formation. A relationship was found to exist between the temperature during deposition and the film composition with a maximum nickel content reached at approximately 530 °C. The effect of annealing both the nickel-rich and the boron-rich films was studied by SEM, XRD, and electron diffraction experiments. SEM data for the annealed boron-rich films showed the formation of perfect hexagonal crystals in a channelled columnar matrix. Electron diffraction data showed that this crystalline phase is hexagonal Ni_7B_3 isolated in a Ni_3B matrix. The as-deposited nickel-rich films were found by XRD studies to be primarily pure nickel, containing relatively small amounts of the Ni_3B phase relative to the pure nickel phase. This has been attributed to the precipitation of boron-rich phases as very small crystallites at the grain boundaries of the pure nickel material. XRD spectra for the boron-rich films showed that the films consisted of Ni_3B with no pure nickel observed. Annealing of these films did not result in the formation of pure nickel phases in the XRD spectra.

Introduction

In recent years, the formation of transition metal boride thin films has received increasing research attention. Interest in the preparation,[2] theoretical modeling,[3] and solid-state characteristics[4] of these metal borides is primarily due to their unique physical properties among solid-state materials and to their wide structural diversity. Metal borides are typically extremely refractory materials, frequently with melting points far in excess of that found for the pure metal. In addition, they are exceptionally hard materials which are resistant to attack even in the most harsh chemical environments.[4] The transition metal borides are also known to be good electrical conductors, with resistivities occasionally lower than the corresponding pure metals (i.e., LaB_6), and some even become superconducting at low temperatuers. Thus, metal borides have found increased use not only in traditional applications such as hard coatings for cutting tools[5] but also in thermally and chemically taxed aerospace components,[6] high-energy optical systems,[7] thermionic emitters, and new magnetic materials.[8]

(1) Part 1: Glass, J. A., Jr.; Kher, S.; Spencer, J. T. *Thin Solid Films* **1992**, *207*, 15. Part 2: Glass, J. A., Jr.; Kher, S. S.; Spencer, J. T. *Chem. Mater.*, previous paper in this issue.

(2) (a) Thompson, R. *Prog. Boron Chem.* **1970**, *2*, 173. (b) Schwarzkopf, P.; Kieffer, R.; Leszynski, W.; Benesovsky, K. *Refractory Hard Metals, Borides, Carbides, Nitrides, and Silicides*; MacMillan: New York, 1953. (c) Aronsson, B.; Lundstrom, T.; Rundqvist, S. *Borides, Silicides and Phosphides*; Wiley: New York, 1965. (d) *Boron and Refractory Borides*; Matkovick, V. I., Ed.; Springer-Verlag: New York, 1977. (e) Samsonov, G. V.; Goryachev, Y. M.; Kovenskaya, B. A. *J. Less.-Common Met.* 1976, *47*, 147. (f) Lipscomb, W. N. *J. Less.-Common Met.* 1981, *82*, 1. (g) Etourneau, J.; Hagenmuller, P. *Philos. Mag.* **1985**, *52*, 589.

(3) (a) Minyaev, R. M.; Hoffmann, R. *Chem. Mater.* **1991**, *3*, 547. (b) Burdett, J, K.; Canadell, E. *Inorg. Chem.* **1988**, *27*, 4437. (c) Mohn, P.; Pettifor, D. G. *J. Phys. C: Solid State Phys.* **1988**, *21*, 2829. (d) Mohn, P. *J. Phys. C: Solid State Phys.* **1988**, *21*, 2841. (e) Burdett, J. K.; Canadell, E.; Miller, G. J. *J. Am. Chem. Soc.* **1986**, *108*, 6561. (f) Pettifor, D. G.; Podloucky, R. *J. Phys. C: Solid State Phys.* **1986**, *19*, 315. (g) Armstrong, D. R. *Theor. Chim. Acta* **1983**, *64*, 137. (h) Armstrong, D. R.; Perkins, P. G.; Centina, V. E. *Theor. Chim. Acta* **1983**, *64*, 41. (i) Ihara, H.; Hirabayashi, M.; Nakagawa, H. *Phys. Rev. B: Solid State Phys.* **1977**, *B16*, 726. (j) Perkins, P. G.; Sweeney, A. V. J. *J. Less.-Common Met.* **1976**, *47*, 165. (k) Liv, S. H.; Koop, L.; England, W. B.; Myron, H. W. *Phys. Rev. B: Solid State Phys.* **1975**, *B11*, 3463.

(4) Samsonov, G. V. *Handbook of High-Temperature Materials, No. 2 Properties Index*; Plenum Press: New York, 1964.

(5) (a) Mullendore, A. E.; Pope, L. W. *Thin Solid Films* **1987**, *153*, 267. (b) Skibo, M.; Greulich, F. A. *Thin Solid Films* **1984**, *113*, 225. (c) Campbell, A. N.; Mullendore, A. W.; Hills, C. R.; Vandersande, J. B. *J. Mater. Sci.* **1988**, *23*, 4049.

(6) (a) Patterson, R. J. U.S. Patent No. 3, 499,799, 1970. (b) Lewandowski, R. S. U.S. Patent No. 4,522,849, 1985. (c) Branovich, L. E.; Fitzpatrick, W. B. P.; Long, M. L.; Jr. U.S. Patent No. 3,692,566, 1972.

(7) Knittl, Z. *Optics of Thin Films*; Wiley and Sons: New York, 1976.

(8) (a) Bakonyi, I. *J. Magn. Magn. Mater.* **1988**, *73*, 171. (b) Mutlu, R. H.; Aydinuraz, A. *J. Magn. Magn. Mater.* **1987**, *68*, 328. (c) Lundquist, N.; Myers, H. P.; Westin, R. *Philos. Mag.* **1962**, *7*, 1187. (d) Kaul, S. N.; Rosenberg, M. *Phys. Rev.* **1982**, *B25*, 5863. (e) Bakonyi, I.; Panissod, P.; Durand, J.; Hasegawa, R. *J. Non-Cryst. Solids* **1984**, *61/62*, 1189.

0897-4756/92/2804-0538$03.00/0

Metal boride phases have been reported for essentially all of the metallic elements including the lanthanides and actinides. The structures of these materials vary from metal-rich borides with isolated boron atoms in a metal lattice, such as Mn_4B and Ni_3B, to the boron-rich materials with three-dimensional lattices of linked boron icosahedra, such as YB_6 and AlB_{12}.[2] The tendency of boron to catenate as the boron content in these phases increases results in the unique diversity of structural types between these two structural extremes. Other structural types frequently encountered with the metal borides include zigzag boron chains, single- and double-branched boron chains, and two-dimensional boron lattices. Because of this structural diversity, recent efforts have been made to understand the electronic structure of these materials on a theoretical basis.[3]

Metal boride coatings have in the past been primarily prepared by the electrolytic deposition of the materials either from fused salts[2] or from solution.[9] Because of the high temperatures required and the refractory nature of the products, pure metal boride materials have been difficult to prepare in these fashions. The production of high-purity metal boride materials for demanding technological applications, therefore, requires a suitable materials technology for the preparation of pure epitaxial structures. Chemical vapor deposition (CVD) technology has recently been shown to be one of the most effective current techniques for the deposition of clean thin films.[10] CVD provides numerous advantages over traditional depositional methods, including (1) clean and controllable stoichiometric deposition processes (resultant films are typically only dependent on the choice of precursor material and easily controlled deposition conditions), (2) superior thin-film uniformity, (3) potential for pattern deposition with sharp boundary features through "real-time" processes, (4) lower temperature depositions, (5) significant migration reduction at film–substrate interfaces, (6) experimental ease of deposition from starting precursor materials, (7) facile application to main-group-containing materials, and (8) the facility for larger scale production processes. In addition, many of the non-CVD processes are carried out at elevated temperatures which frequently cause severe interlayer diffusion and result in vague interlayer junctures. In recognition of these advantages, considerable effort has been directed toward employing CVD techniques for manufacturing refractory semiconductor thin films.[11] The advantages make CVD technology the methodology of choice for the formation of desired refractory thin-film materials.

One of the newest families of precursor compounds to be investigated for CVD applications for the formation of a metallic thin films are the boron-containing compounds.[6,12d] The chemical properties of many of these species provide unique solutions to several difficult problems frequently encountered with traditional MOCVD source compounds.[12] In this paper we report the results of our investigations into the formation, characterization and properties of nickel boride thin films arising from the chemical vapor deposition of boron-containing precursor cluster compounds. The nickel borides were chosen for investigation due to their structural diversity and potential applications, especially as a magnetic material and refractory coating.

The chemical vapor deposition of nickel boride thin films has recently been reported from the binary mixture of $Ni(CO)_4$ and diborane(6), B_2H_6, in an argon/carbon monoxide carrier.[5] This deposition is similar to the CVD formation of Ni_3C form $Ni(CO)_4$ and CO.[13] In addition, group IV borides (Ti, Zr, and Hf) have been prepared by CVD from either the reduction of a metal halide with a boron trihalide compound by hydrogen at 1200 °C[5] or by the lower temperature deposition of metal borohydride complexes.[14] The control of the stoichiometry in multicomponent films prepared by chemical vapor deposition techniques has, in the past, frequently relied on varying the ratio of several individual source compounds in the vapor phase. These source materials typically deposit at significantly different rates on the substrate at a given temperature, often making the formation of a homogeneous film difficult to achieve. Frequently the individual source materials, such as $Ni(CO)_4$ and B_2H_6 are relatively expensive and extremely toxic and flammable reagents. An alternative method which provides stoichiometric control in the formation of strain-free, conformal thin-film materials was thus highly desirable and the subject of this paper.

Experimental Section

Physical Measurements. FT-IR spectra in the range 400–4000 cm^{-1} were measured on a Mattson Galaxy 2020 spectrometer and were referenced to the 1601.8-cm^{-1} band of polystyrene. Scanning electron micrographs (SEM) were obtained on an ETEC autoscan instrument in the Center for Ultrastructure Studies of the S.U.N.Y. College of Environmental Science and Forestry. Photographs were recorded on either Kodak Ektapan 4162 or Polaroid PN 55 film. Energy-dispersive X-ray analyses (EDXA) were obtained on a Kevex 7500 Microanalyst System. The X-ray diffraction spectra (XRD) were measured on a Phillips APD 3520 powder diffractometer equipped with a PW 1729 X-ray generator and a PW 1710 diffractometer control system. Copper Kα radiation and a graphite single-crystal monochromator were employed in the measurements reported here. The Auger electron spectra (AES) were measured on either a Perkin-Elmer PHI 595 scanning Auger microprobe instrument in the Electronics Laboratory of General Electric Company, Syracuse, NY, or a similar instrument at the U.S.A.F. Rome Laboratory, Rome, NY. Depth profiles were obtained by alternately sputtering the top of the sample with an Ar^+ ion beam and measuring the AES spectrum. The profiles were obtained using a 10-kV, 150-nA rastered electron beam and an argon ion beam at 3.5 kV and 860 nA/mm^2. The concentrations for all elements except hydrogen and helium were measured in the spectra. Atomic absorption (AA) measurements were made on a Perkin-Elmer 2380 atomic absorption spectrophotometer operating with a Perkin-Elmer nickel lamp. Nickel

(9) (a) Duncan, R. N.; Arney, T. L. *Plating Surf. Fin.* **1984**, 49. (b) Goldie, W. *Metallic Coating of Plastics*; Electrochemical Publications Ltd.: London, 1968; Vol. 1. (c) Flechon, J.; Voiriot, F. *Bull. Soc. Chim. Soc. Fr.* **1963**, *93*, 509. (d) Flechon, J.; Voiriot, R. *J. Phys.* **1963**, *24*, 767. (e) Flechon, J.; Kuhnast, F. A. *J. Chim. Phys.* **1972**, *69*, 1136. (f) Petrov, Y. N.; Kovalev, V. V.; Markus, M. M. *Dokl. Akad. Nauk SSSR* **1971**, *198*, 118. (g) Ivanov, M. V.; Moiseev, V. P.; Gorbunova, K. M. *Dokl. Akad. Nauk SSSR* **1970**, *194*, 367. (h) Gorbunova, K. M.; Ivanov, M. V.; Moiseev, V. P. *J. Electrochem. Soc.* **1973**, *20*, 613. (i) Hedgecock, N.; Tung, P.; Schlesinger, M. *J. Electrochem. Soc.* **1975**, *122*, 866.

(10) (a) Dowben, P. A.; Spencer, J. T.; Stauf, G. T. *Mater. Sci. Eng. B* **1989**, *B2*, 297. (b) Leys, M. R. *Chemtronics* **1987**, *2*, 155. (c) Davies, G. J.; Andrews, D. A. *Chemtronics* **1988**, *3*, 3. (d) Jones, A. C.; Roberts, J. S.; Wright, P. J.; Oliver, P. E.; Cockayne, B. *Chemtronics* **1988**, *3*, 152.

(11) Shmartsev, Y. V.; Valov, Y. A.; Borschevskii, A. S. *Refractory Semiconductor Materials*; Goryunova, N. A., Nasledov, D. N.; Eds.; Plenum Publishing: New York, 1966.

(12) (a) Glass, J. A.; Kher, S.; Hersee, S. D.; Ramseyer, G. O.; Spencer, J. T. *Mater. Res. Soc. Symp. Proc.* **1991**, *204*, 397. (b) Amini, M. M.; Fehlner, T. P.; Long, G. J.; Politowski, M. *Chem. Mater.* **1990**, *2*, 432. (c) Kim, Y.-G.; Dowben, P. A.; Spencer, J. T.; Ramseyer, G. O. *J. Vac. Sci. Technol. A* **1989**, *7*, 2796. (d) Mazurowski, J.; Baral-Tosh, S.; Ramseyer, G.; Spencer, J. T.; Kim, Y.-G.; Dowben, P. A. *Mater. Res. Soc. Symp. Proc.* **1991**, *190*, 101. (e) Zhang, Z.; Kim, Y.-G.; Dowben, P. A.; Spencer, J. T. *Mater. Res. Soc. Symp. Proc.* **1989**, *131*, 407.

(13) Vainshtein, B. K. *Structure Analysis by Electron Diffraction*; Pergamon: New York, 1964; p 335.

(14) (a) Jensen, J. A.; Gozum, J. E.; Pollina, D. M.; Girolami, G. S. *J. Am. Chem. Soc.* **1988**, *110*, 1643. (b) Gozum, J. E.; Girolami, G. S. *J. Am. Chem. Soc.* **1991**, *113*, 3829.

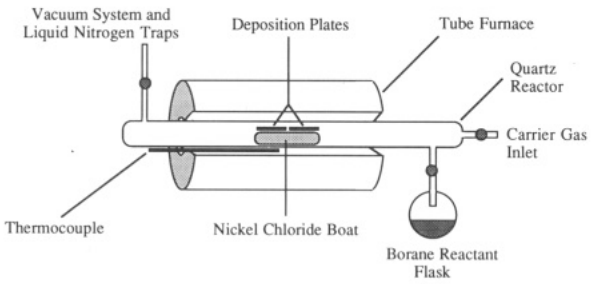

Figure 1. Experimental setup for the formation of nickel boride thin film materials from boron-containing source compounds using a "hot wall" reactor system.

analyses were performed using a wavelength of 232 nm.

Materials. All solvents used were reagent grade or better. The pentaborane(9), B_5H_9, was from our laboratory stock. All compounds were prepared and manipulated using standard vacuum line techniques.[15] All compounds were characterized by multinuclear high-resolution NMR and FT-IR spectroscopy, and the results were compared to literature values to confirm the authenticity of the samples. The anhydrous nickel chloride was commercially available (Strem) and was used as received. Standard nickel boride samples (Ni_3B) were purchased from Cerac and used as received. The nickel AA standard solution (for the construction of the AA calibration curves) was purchased from Aldrich.

Depositions. The depositions were performed in a medium-high vacuum hot wall deposition apparatus (1×10^{-6} Torr ultimate vacuum) equipped with a chromel–alumel thermocouple. A schematic diagram for the experimental setup is shown in Figure 1. In a typical experiment, 1.0 g (7.7 mmol) of anhydrous (99%) nickel(II) chloride was placed in the quartz boat in the hot wall deposition system using inert atmosphere techniques.[15] A boron-source reservoir containing either freshly sublimed *nido*-decaborane(14), $B_{10}H_{14}$, or vacuum-distilled *nido*-pentaborane(9), B_5H_9, was connected to the reactor. The borane reservoir flask was maintained at a constant temperature during the entire experiment by use of an external temperature bath jacketing the flask (22 °C for decaborane(14) and −78 °C for pentaborane(9)). Control of the source flow in the system was achieved through the use of narrow-bore Teflon vacuum stopcocks (0–4 mm) and by cooling the precursor flask using an external slush bath to lower its vapor pressure.[15] The entire deposition apparatus was evacuated to 1×10^{-5} Torr. The reactor was slowly heated to 500 °C under dynamic vacuum. After obtaining a stable temperature, the needle valve to the borane reservoir flask was opened to allow a vapor of the borane to pass over the hot $NiCl_2$ while under dynamic vacuum conditions. The unreacted borane and other reaction byproducts were trapped downstream in a liquid nitrogen cooled trap. The pressure in the reactor during the deposition was approximately 1 Torr. The deposition was continued for 1 h, during which time a silvery metallic thin film coated the walls of the reactor and the deposition substrates held above the $NiCl_2$ boat (Figure 1). The stopcock to the borane flask was then closed. The reactor was then allowed to cool to room temperature by opening the top portion of the split furnace (see Figure 1). In experiments in which the films were thermally annealed after the deposition, the reactor was slowly heated to 830 °C and maintained at that temperature for 35–40 h. The reactor was then allowed to cool slowly to room temperature over 10–12 h while constant pumping was maintained. The reactor was filled with dry nitrogen and the film was removed from the system for further study. The films thus prepared were typically very highly specular, flexible, and very hard materials.

Analysis. The films were typically analyzed by scanning electron microscopy (SEM), energy-dispersive X-ray analysis (EDXA), Auger electron spectroscopy (AES), and X-ray thin-film diffraction (XRD). For the SEM and EDXA studies of a film, the film was mounted on an aluminum stub with double-sided tape, and the edges were coated using carbon paint to provide a conductive contact between the sample and the aluminum stub. For the XRD studies, the films were mounted on a glass microscope slide using double-sided adhesive tape.

The films were analyzed for nickel content by atomic absorption spectrophotometry (AA). In a typical AA analysis, a known amount of film was dissolved in 10 mL of a hot 6.1 M HNO_3 solution. The solution, upon cooling to room temperature, was diluted to exactly 100 mL. The AA measurements on the unknown samples were compared to a standard calibration curve to determine the percent nickel in the film sample.[16] Since the boron in the nickel boride films was oxidized to boric acid during the sample preparation, the effect boric acid on the AA nickel determination was evaluated. This possible interference in the analysis was determined by running two sets of standard nickel solutions, one with boric acid added and the other set without boric acid. In these experiments, the addition of large quantities of boric acid had no effect upon the observed nickel analysis.

The relationship between the temperature of the deposition and the elemental composition of the films at constant borane flow rates and reactor vacuum conditions was studied using a slightly modified deposition procedure. In this study, the nickel source reservoir was charged with 1.0 g (7.7 mmol) of $NiCl_2$. The reactor was then heated and maintained at the desired temperature during the deposition. The pentaborane(9) was admitted into the reactor, and the deposition was allowed to proceed for 1 h. The flow of the pentaborane(9) into the reactor was kept the same for each of the depositions in this study. The borane flow was stopped after 1 h, and the reactor cooled to room temperature. Film samples were consistently removed from the same location in the reactor for each measurement. The elemental compositions of the films were determined by AA analyses.

Results and Discussion

Metal Boride Thin-Film Formation Studies. The formation of thin films of metal-rich and boron-rich phases of nickel boride from boron-containing precursor compounds by a cluster deposition process was achieved through the vapor-phase reaction of the boron cluster compounds, *nido*-pentaborane(9), B_5H_9, and *nido*-decaborane(14), $B_{10}H_{14}$, with anhydrous nickel chloride, $NiCl_2$, in a hot-walled, vacuum deposition system. A schematic diagram for this reactor is shown in Figure 1. Films were formed both on substrates suspended in the cavity of the reactor and on the walls of the reactor system itself in the hot zone. The films were formed on a variety of amorphous and monolithic substrates including copper, SiO_2-(100), GaAs(100), tantalum, Si(100), fused silica (quartz), and Pyrex. Substrate-free materials were obtained by peeling the materials from the walls of the reactor. The onset of thin-film formation (~440 °C) occurred at relatively low temperatures. The metal-rich films were all highly specular and, in the case of the substrate-free materials, were also found to be very flexible and strong. The nickel-rich annealed thin films were so hard that they were exceedingly difficult to cut with a stainless steel blade. Film thicknesses of up to 3 μm were prepared in our experiments by controlling the flow rate of the volatile borane cluster into the reactor (primarily by controlling the temperature of the borane reservoir using an external cooling bath), by controlling the substrate temperature, or by regulating the precursor exposure time to the substrate. Typical deposition rates of 1 μm/h were observed, although higher rates were readily achieved by using higher borane flow rates. The boron-rich materials, in contrast, tended to be dull grey materials which were much more brittle than the metal-rich films.

The films were typically characterized by energy-dispersive X-ray analysis (EDXA), Auger electron spectros-

(15) Shriver, D. F.; Drezdzon, M. A. *The Manipulation of Air-Sensitive Compounds*; Wiley-Interscience: New York, 1986.

(16) Willard, H. H.; Merritt, L. L., Jr.; Dean, J. A.; Steele, F. A., Jr. *Instrumental Methods of Analysis*; Wadsworth Publishers: Belmont, CA, 1981.

Table I. Selected Deposition Data for Typical Nickel Boride Thin Films Derived from Boron-Containing Precursor Compounds

film no.	source compound	substrate	substrate temp, °C	source temp, °C	deposition duration, h	nickel content
1	$B_{10}H_{14}$	Pyrex	444	22	3	90.4[a]
2	$B_{10}H_{14}$	Pyrex	566	22	3	56.6[a]
3	$B_{10}H_{14}$	Pyrex	505	22	3	86.8[a]
4	$B_{10}H_{14}$	Pyrex	536	22	3	81.9[a]
5	$B_{10}H_{14}$	Pyrex	491	22	3	94.3[b]
6	B_5H_9	Si(100)	501	-78	3	85.0[b]
7	B_5H_9	copper	500	-78	3	66.0[b]
8	B_5H_9	Ta	499	-78	3	86.6[a]
9	B_5H_9	Pyrex	460	-78	3	81.1[a]
10	B_5H_9	Pyrex	500	-78	3	66.0[b]
11	B_5H_9	Pyrex	520	-78	3	90.5[a]
12	B_5H_9	Pyrex	601	-78	3	76.8[a]

[a] Determined by atomic absorption analysis. [b] Determined by Auger electron analysis.

copy (AES), scanning electron microscopy (SEM), X-ray diffraction (XRD), transmission electron microscopy (TEM) and electron diffraction experiments. Selected deposition data and experimental parameters for the formation of typical nickel boride thin films from these boron-containing precursor compounds are given in Table I.

Pentaborane(9) has the advantage of being a highly volatile, thermally stable liquid [vapor pressure (at 25 °C) = 209 Torr][17a] and can therefore be more easily controlled in a flow system than decaborane(14) [vapor pressure (at 60 °C) = 1 Torr].[17b,c] Decaborane(14) has the advantage of being an air-stable material at room temperature while pentaborane(9) reacts violently with air.[18] Both of these boranes, however, gave very similar depositional results.

Metal Boride Compositional Dependence Studies. The stoichiometric composition of the films (nickel:boron ratio) was controlled by regulating the deposition temperature, the borane flow rate into the reactor, and the base vacuum conditions during the film formation. Materials with nickel contents as high as >99.9% (no boron detected) and as low as 56.6% were prepared. When the borane flow rate and reactor vacuum conditions were held constant, a relationship was found to exist between the temperature of the deposition and the elemental composition of the films. This correlation is shown in Figure 2. The onset of deposition occurred at approximately 440 °C with the formation of relatively boron-rich films. As the temperature of deposition increased, the nickel content also increased and reached a maximum near 530 °C. After this maximum, the nickel content was found to decrease with increasing deposition temperature.

The observed deposition characteristics can be generally rationalized by considering the gas-phase composition of the reaction system. In these experiments, the vapor-phase concentration of the borane in the reactor was held constant while the vapor pressure of the nickel chloride within the reaction chamber, however, varied with the temperature of the reactor since the nickel chloride reservoir was located entirely within the hot zone of the furnace. The vapor pressure of the nickel chloride in the gas phase is given by the expression $\log P_{mm} = 12.051 - (11{,}499/T)$.[19] At lower temperatures, the gas-phase concentration of the

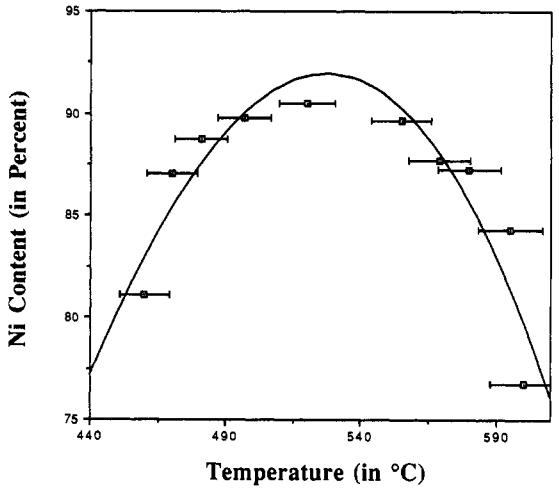

Figure 2. Plot of the nickel content versus the deposition temperature for nickel boride thin films as determined by atomic absorption elemental analysis (error bars indicate 2% of the coordinate). The films were prepared on a quartz substrate using a *nido*-pentaborane(9), B_5H_9, borane source kept at -78 °C during the deposition.

borane cluster is significantly larger than the nickel chloride concentration. Under these gas-phase conditions, boron-rich films are formed. As the temperature of the reactor increases, the concentration of the nickel chloride in the gas phase also increases relative to the concentration of the borane component. The result is films in which the nickel content steadily increases. At still higher temperatures, the nickel content of the films was observed to first stabilize and then decrease. Two mechanistic pathways can be postulated to account for this effect. In the first explanation, nickel chloride is known to vaporize primarily as $NiCl_2$ at lower temperatures. At approximately 400 °C, however, a disproportionation reaction of the $NiCl_2$ is initiated in which very small amounts of the subhalide NiCl forms.[20] As the reactor temperature increases, the relative importance of the disproportion reaction increases until it becomes the dominant reaction which results in primarily NiCl and other subhalides as the primary volatilized species (with no Cl_2 produced).[20] The rates of reaction of $NiCl_2$ and NiCl with borane clusters and the greatly varying vapor pressures of these species, and thus the vapor phase nickel content, result in a decreased nickel content of the films with increasing deposition temperature. A second possible explanation for the observed nickel content reduction at elevated temperatures is that the surface of the nickel chloride reservoir becomes contaminated with

(17) (a) Wirth, H. E.; Palmer, E. D. *J. Phys. Chem.* **1956**, *60*, 914. (b) Hurd, D. T.; Safford, M. M. U.S. Patent No. 2,588,559, June 26, 1954. (c) Safford, M. M.; Hurd, D. T. U.S. Patent No. 2,558,561, June 26, 1954.

(18) (a) Muetterties, E. L. *Boron Hydride Chemistry*; Academic Press: New York, 1975. (b) Lipscomb, W. N. *Boron Hydrides*; Benjamin: New York, 1963. (c) Onak, T. In *Comprehensive Organometallic Chemistry*; Wilkinson, G., Stone, F. G. A., Abel, E., Eds.; Pergamon: Oxford, 1982; Chapter 5.4.

(19) Nicholls, D. In *Comprehensive Inorganic Chemistry*; Bailar, J. C.; Emeleus, H. J.; Nyholm, R.; Trotman-Dickenson, A. F., Eds.; Pergamon: Oxford, 1973; Chapter 42, p 1126.

(20) (a) Scheer, M. D.; Klein, R.; McKinley, J. D. *Surf. Sci.* **1972**, *30*, 251. (b) Dowben, P. A. Ph.D. Thesis, Cambridge University, 1981.

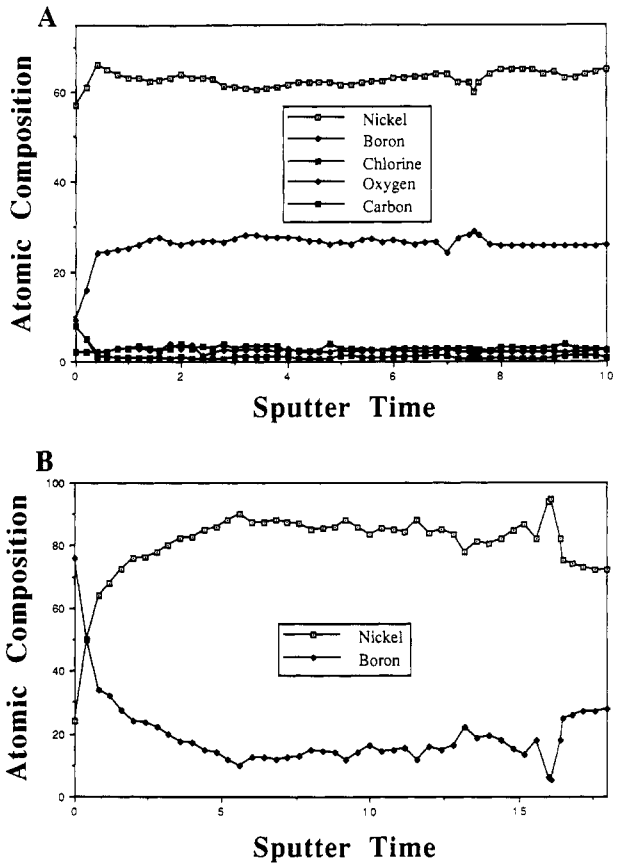

Figure 3. Representative Auger electron spectra for nickel boride thin films deposited using a *nido*-pentaborane(9), B_5H_9, source kept at −78 °C during the deposition. The depth profiles were constructed from Auger electron spectra as the film was sputtered using Ar^+ ion milling. Sputter times are given in minutes, and the atomic compositions are given in percent. (a) Nickel boride film deposited at 500 °C on Pyrex. (b) Nickel boride film deposited at 497 °C on fused silica (quartz).

a refractory layer of either nickel boride or native boron. As this source reservoir blanketing increases, the relative nickel chloride concentration in the gas phase again decreases as smaller portions of the reservoir are left uncontaminated. This surface contamination has been observed experimentally in the higher temperature ranges as a black layer coating the surface of the reservoir. It seems reasonable to suggest that the observed nickel content decrease may actually involve both of these proposed mechanisms.

Thin-Film Characterization. Energy-dispersive X-ray analysis (EDXA) of the films clearly showed only the intense signals from nickel at 7.477-keV ($K\alpha_1$) and those from the substrate. No other heavy elements, such as chloride, were detected. Since the film compositions for boron and the other lighter elements were not obtained directly from our EDXA data, the Auger electron spectra (AES) were measured to determine the complete film composition as a function of thickness. The results of the Auger electron depth profile for two typical NiB films are shown in Figure 3. The surface layer was found to be contaminated with a small amount of carbon but dropped to within the AES detection limits very rapidly. The contamination of the surface by chlorine was also observed and found to drop very rapidly to the AES detection limit in the bulk sample. In each sample, the film composition was found to be uniform with depth and showed no contamination from carbon to oxygen in the bulk samples. The absence of other heavy elements, such as chloride, in the bulk sample was confirmed in the AES measurements. A FT-IR spectrum of a ground film showed no B–H vibrations (characteristically near 2500 cm^{-1}),[21] confirming the absence of intact borane clusters or cluster fragments trapped in the films.

Scanning electron microscopy provided detailed pictures of the morphology of the nickel boride thin films. The SEM photomicrographs of selected films prepared from depositions involving nickel chloride and pentaborane(9) are shown in Figure 4. The as-deposited nickel-rich films were found to be relatively smooth, conformal materials which displayed very small surface voids (Figure 4a). Void formation in films formed from physical vapor deposition techniques are typically attributed to shadowing effects.[22] In other deposition processes, because depositions typically occur at sufficiently higher temperatures, the surface mobility of the material being deposited effectively averts void formation by this shadow mechanism. In the CVD nickel boride films reported here, however, the relatively low temperatures and the presumed lower surface mobility of the deposited boride phases permitted the formation of voids by the shadowing process. The observation of very small surface voids with irregular shapes in the boron-rich films (Figure 4a) provides further support for the operation of this mechanism. These structures are also parallel to the deposition direction and are typical of vapor-deposited metal films in which the substrate temperature is significantly lower than the melting point of the pure metal.[5b,23] Annealing these films resulted in the formation of a material with rather uniform grain sizes (Figure 4b). The as-deposited boron-rich materials were very similar in surface morphology to those of the nickel-rich materials. Upon annealing the boron-rich materials, however, significant crystalline modifications were observed (Figure 4c–f). Perfect hexagonal crystals in a channelled Ni_3B (by XRD) columnar matrix were observed in these films. EDXA elemental mapping of the crystals showed that they contained only nickel (boron could not be detected by our energy-dispersive X-ray analysis). To identify these crystalline materials, electron diffraction patterns were analyzed and compared with the diffraction data for the known nickel boride phases.[27–32] The data from these spectra show that this crystalline phase is hexagonal

(21) Electron diffraction data (selected most intense peaks): observed for hexagonal Ni_7B_3 (*d* spacings given in angstroms and the *hkl* assignments are given in the parentheses for each reflection); d_{obs} = 6.024 (100), $d_{lit.}$ = 6.036; d_{obs} = 3.482 (110), $d_{lit.}$ = 3.485; d_{obs} = 3.021 (200), $d_{lit.}$ = 3.018; d_{obs} = 2.252 (210), $d_{lit.}$ = 2.281; d_{obs} = 2.008 (300), $d_{lit.}$ = 2.012; d_{obs} = 1.732 (220), $d_{lit.}$ = 1.742; d_{obs} = 1.508 (400), $d_{lit.}$ = 1.509; d_{obs} = 1.199 (500), $d_{lit.}$ = 1.207; d_{obs} = 1.155 (330), $d_{lit.}$ = 1.16 (calcd); d_{obs} = 1.131 (420), $d_{lit.}$ = 1.139 (calcd); d_{obs} = 1.001 (600), $d_{lit.}$ = 1.006 (calcd); d_{obs} = 0.864 (700), $d_{lit.}$ = 0.862 (calcd); d_{obs} = 0.856 (530), $d_{lit.}$ = 0.861 (calcd); d_{obs} = 0.753 (800), $d_{lit.}$ = 0.754 (calcd); d_{obs} = 0.746 (720), $d_{lit.}$ = 0.736 (calcd); d_{obs} = 0.678 (730), $d_{lit.}$ = 0.678 (calcd); d_{obs} = 0.663 (820), d_{lit} = 0.658 (calcd); d_{obs} = 0.597 (920), $d_{lit.}$ = 0.594 (calcd); d_{obs} = 0.572 (10 10), $d_{lit.}$ = 0.57 (calcd); d_{obs} = 0.562 (930), $d_{lit.}$ = 0.557 (calcd); d_{obs} = 0.54 (760), $d_{lit.}$ = 0.535 (calcd). (a) Machizaud, F.; Kuhnast, F. A.; Flechon, J.; Auguin, B.; Defresne, A. *J. Phys.* **1981**, *42*, 97. (b) Machizaud, F., personal communication. (c) Complete electron diffraction analysis: Kher, S. S.; Spencer, J. T. *Mater. Res. Soc. Symp. Proc.* **1992**, R5.9, in press.

(22) Movchan, B. A.; Demchishin, A. V. *Fiz. Met.* **1977**, *28*, 83.

(23) Leamy, H. J.; Dirks, A. G. *J. Appl. Phys.* **1978**, *49*, 3430.

(24) Azaroff, L. V.; Buerger, M. J. *The Powder Method in X-ray Crystallography*; McGraw-Hill: New York, 1958.

(25) Wodniecka, B.; Wodniecka, P.; Krolas, K.; Thome, L. *J. Phys. Fr.: Met. Phys.* **1986**, *16*, 1629.

(26) (a) Hoffmann, S. In *Surface Segregation Phenomena*; Dowben, P. A., Miller, A., Eds.; CRC Press: Boca Raton, FL, 1990; Chapter 4. (b) Uebing, C.; Viefhaus, H.; Grabke, H. J. *Ibid.*; Chapter 9.

(27) Goldschmidt, H. J. *Interstitial Alloys*; Plenum Press: New York, 1967; p 264.

(28) Rundqvist, S. *Acta Chem. Scand.* **1958**, *12*, 658.

(29) Fruchart, A.; Michel, A. *Compt. Rend.* **1957**, *245*, 171.

(30) Andersson, L. H.; Kiessling, R. *Acta Chem. Scand.* **1950**, *4*, 160.

(31) Rundqvist, S. *Acta Chem. Scand.* **1959**, *13*, 1193.

(32) Blume, P. *J. Phys. Rad.* **1952**, *13*, 430.

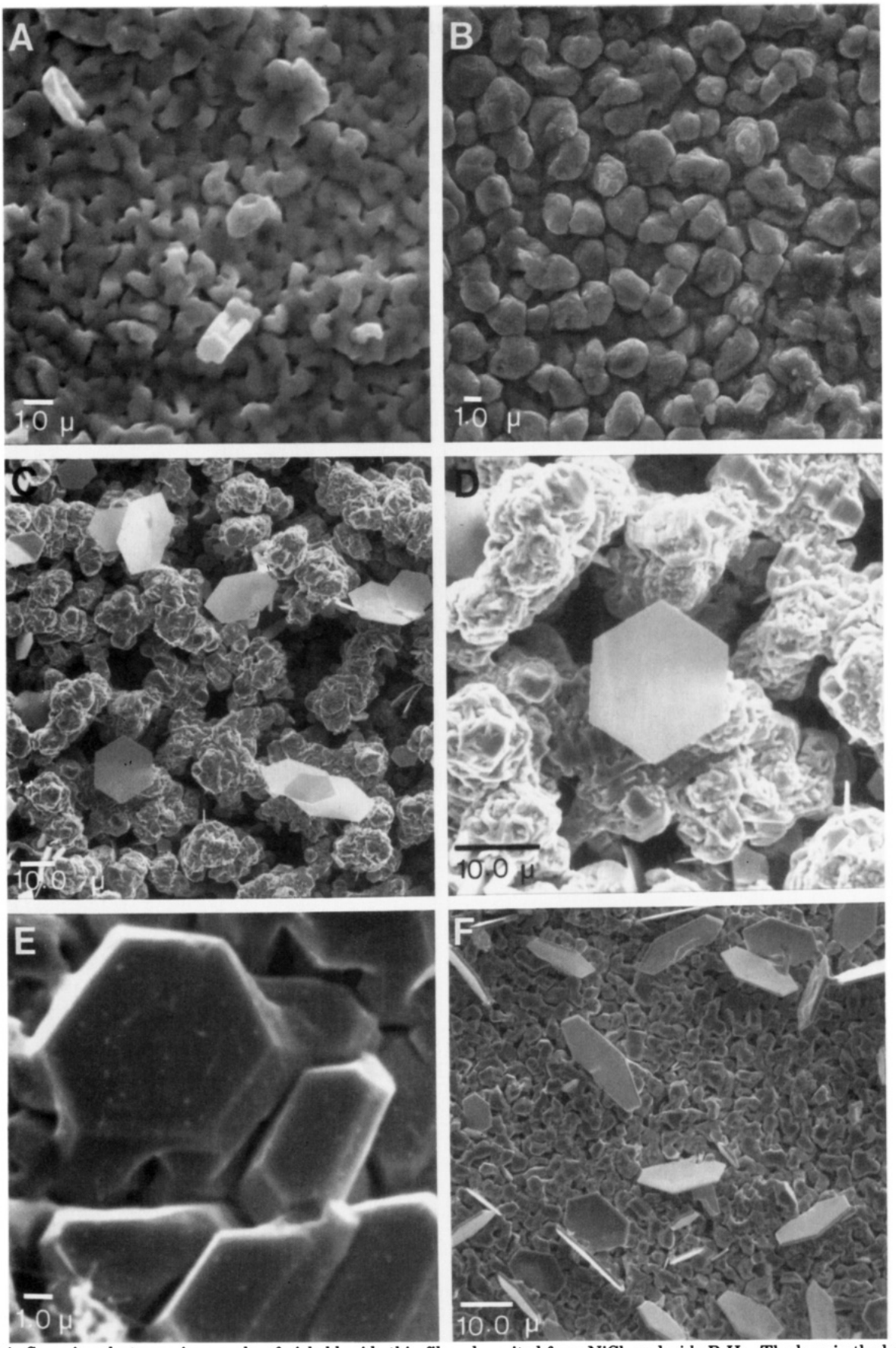

Figure 4. Scanning electron micrographs of nickel boride thin films deposited from $NiCl_2$ and *nido*-B_5H_9. The bars in the lower left corners of each photograph indicate scale. (a) Electron micrograph of an as-deposited nickel-rich thin film (determined by XRD) deposited at 482 °C on Pyrex. (b) Photomicrograph of the nickel-rich thin film shown in (a) that had been vacuum annealed at 750 °C for 15-h postdeposition. (c) Annealed boron-rich thin film (determined by XRD) deposited at 502 °C on fused silica (quartz) and annealed at 830 °C for 38-h postdeposition. (d) Enlargement of one of the Ni_7B_3 hexagonal crystals from (c) in the Ni_3B matrix. (d) Annealed boron-rich thin film (determined by XRD) deposited at 502 °C on GaAs(100) and annealed at 830 °C for 38-h postdeposition. (f) Electron micrograph of Ni_7B_3 crystals in the Ni_3B matrix of an annealed thin film.

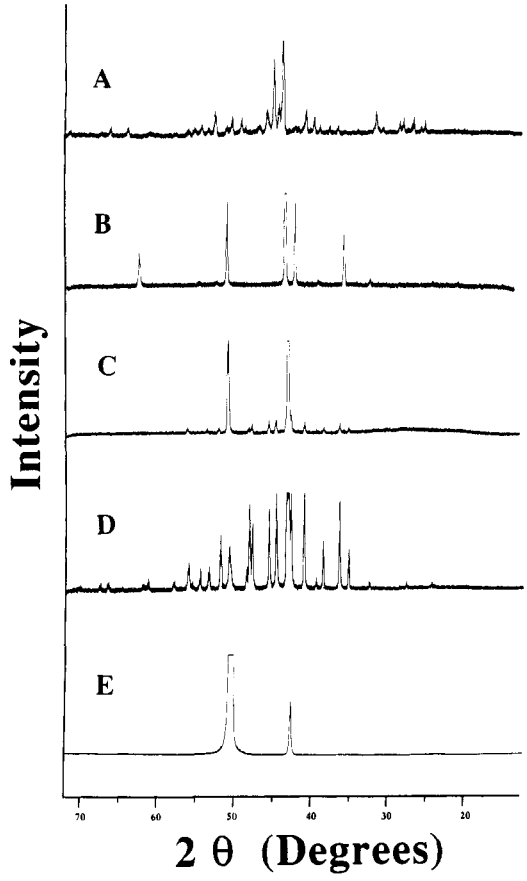

Figure 5. X-ray diffraction spectra for nickel boride thin films deposited on fused silica (quartz) from $NiCl_2$ and *nido*-B_5H_9. The XRD spectra were recorded at room temperature from free-standing films mounted on Pyrex plates. The largest peak in each spectrum is cropped in order to display the smaller peaks in each spectrum. (a) Diffractogram of a boron-rich thin film deposited at 502 °C and annealed at 830 °C for 38-h postdeposition. (b) Diffractogram of nickel-rich thin film deposited at 482 °C and annealed at 750 °C for 15-h postdeposition. This diffractogram is essentially identical to that of a commerically obtained pure nickel foil (Aldrich) that had been similarly annealed. (c) Diffractogram of an as-deposited nickel-rich thin film deposited at 482 °C. The diffractogram clearly shows the presence of both pure nickel and the Ni_3B nickel boride phase. (d) Diffractogram of a commercially obtained Ni_3B powder (Cerac). (e) Diffractogram of a commercially obtained pure nickel foil (Aldrich).

Ni_7B_3.[21] These materials apparently grew from the Ni_3B background matrix during the high-temperature annealing process.

XRD studies of both the as-deposited and annealed nickel-rich and boron-rich films have allowed for the identification of the phases formed during the deposition and the nature of possible phase changes during the annealing process. Selected XRD spectra for these films, along with pure nickel and Ni_3B standards, are shown in Figure 5. All the films were found to be polycrystalline materials which gave sharp diffraction lines in the XRD patterns. The as-deposited nickel-rich films were found to be primarily pure nickel containing a small amount of Ni_3B (Figure 5c). Vacuum annealing of these films resulted in an observed decrease in the Ni_3B phase relative to the pure nickel phase. The resulting XRD patterns were virtually identical to annealed pure nickel foil samples (Figure 5b).

The apparent decrease in the Ni_3B phase on annealing may be explained by a metalloid segregation effect. At the relatively high annealing temperature, the boron atoms in the Ni_3B phase are relatively mobile and readily migrate to the grain boundaries of the pure nickel. The boron-rich material, either pure boron or a boron-rich nickel boride phase, precipitates at these grain boundaries as very fine crystallites.[24] This type of segregation and precipitation has been reported both for boron[25] and other main-group systems, such as carbon and sulfur,[26] in metallic matrices. In addition, the formation of the very small grains in the boron-rich material is consistent with the report that the grain size decreases as the boron content in the phase increases.[5b] Severe broadening in the XRD patterns for materials with grain sizes smaller that 100 Å have been reported for CVD nickel boride alloys.[5b] In fact, when crystallite sizes are near 100 Å or smaller, it is typically not possible to distinguish diffraction maxima from the general background signal.[24] It thus appears that the precipitation of boron-rich phases at the grain boundaries in the annealed nickel-rich films are responsible for the observed decrease in the Ni_3B signals in the XRD patterns. The XRD patterns for the boron-rich films, however, showed that the films consisted of Ni_3B with no pure nickel observed. Annealing of these films did not result in the formation of pure nickel phases in the XRD patterns.

We are continuing our investigation of this deposition and phase transition chemistry including the applicability of the process to other metal systems, the mechanism of the deposition and the magnetic properties of the thin film (by torque magnetometry).[12f] This deposition chemistry provides a convenient method for the formation of refractory metal boride thin-film materials with the potential for a variety of applications.

Acknowledgment. We thank Dr. Stephen D. Hersee, Mr. George O. Ramseyer, and Dr. Lois Walsh for their technical assistance and valuable discussions during the course of this work. We thank the National Science Foundation (Grant No. MSS-89-09793), the General Electric Co., the Wright-Patterson Laboratory (Award No. F33615-90-C-5291), and the Industrial Affiliates Program of the Center for Molecular Electronics for support of this work.

Registry No. Ni_7B_3, 11071-48-0; Ni_3B, 12007-02-2; Ni, 7440-02-0.

Supplementary Material Available: Summarized crystallographic data for the nickel–boron phases reported in the literature (2 pages). Ordering information is given on any current masthead page.